Enhancement of magnetic relaxation properties with 3d diamagnetic cations in [ZnIIILnIII] and [NiIIILnIII], LnIII = Kramers lanthanides†

Júlia Mayans,[a] Queralt Saez,[a] Mercè Font-Bardiab,[b,c] and Albert Escuer [a]

a Departament de Química Inorgànica i Orgànica, Secció Inorgànica and Institute of Nanoscience (IN2UB) and Nanotechnology, Universitat de Barcelona, Marti i Franques 1-11, Barcelona-08028, Spain.

b Departament de Mineralogia, Cristal·lografia i Dipòsits Minerals, Universitat de Barcelona, Solé i Sabarís 1-3, 08028 Barcelona, Spain

c Unitat de Difracció de R-X, Centre Científic i Tecnològic de la Universitat de Barcelona (CCiTUB), Universitat de Barcelona, Solé i Sabarís 1-3, 08028 Barcelona, Spain

Albert Escuer: albert.escuer@qi.ub.es

ABSTRACT:

Employing the chiral bi-compartmental Schiff-base ligand H2L obtained from the condensation of (RR) or (SS)-1,2-diphenyl-ethylenediamine and o-vanillin, we report the structural characterization of the discrete dinuclear pairs of enantiomers [NiIIEuIII] 1RR, 1SS and [ZnIIEuIII] 2RR, 2SS and the magnetic properties for the series of complexes [NiIILnIII], Ln = Ce, 3RR; Nd, 4RR; Dy, 5RR; Er, 6RR, Yb, 7SS and [ZnIILnIII], Ln = Ce, 8RR; Nd, 9RR; Dy, 10SS; Er, 11SS and Yb, 12RR in which MII is diamagnetic and LnIII is a Kramers lanthanide. Single crystal X-ray diffraction shows that relevant changes in the [ZnIILnIII] structures are produced after a period in open air (2RRb, 2RRc), evidencing that the lability of the ligands bonded to ZnII can modify the structures that will be correlated to the experimental measurements. The dynamic magnetic measurements showed that the [NiIILnIII] and [ZnIILnIII] derivatives exhibit different behaviors in the relaxation of magnetization especially for oblate and prolate LnIII cations.

..

INTRODUCTION

Research on coordination compounds containing lanthanide cations is a growing field due to their applications as magnetic resonance contrast agents,1,2,5a catalysts in a wide range ofreactions,3 and molecular magnetic coolers (mainly related to GdIII)4 or due to their luminescence properties in the near infrared (NIR)5 or in the visible regions.6 Regarding their interesting property of exhibiting slow relaxation of magnetization7–10 with potential interest in spintronics11 and quantum computing,12 an increasing number of papers have appeared since the discovery made by Ishikawa et al.13 about the magnetic properties of a single TbIII complex. Lanthanides are especially good candidates for the preparation of Single Ion Magnets (SIMs) because the required large anisotropy comes from the single ion contribution. Lanthanide cations allow this feature due to the relatively small radius of the 4f shell, almost isolated from the environment: as a result, the orbital moment remains unquenched and induces spin–orbit coupling in the ground LS term. Although spin–orbit coupling is a crucial factor for magnetic anisotropy, the crystal field also has an important effect on the SIM response of lanthanide compounds as has been postulated recently by Rinehart and Long,14a and, the fine tuning of the crystal field around the cation influences the magnetic behaviour.14b Low coordination numbers, a symmetry as proper as possible and the dilution of the paramagnetic centers to avoid intermolecular interactions are the goals to enhance the magnetic properties by avoiding the Quantum Tunneling of Magnetization (QTM), which is the drawback in lanthanide magnetism. Control of the coordination spheres is not easy for the LnIII cations because of their tendency to prefer large coordination numbers that often yields low symmetry. Magnetic dilution has been largely explored in lanthanide clusters to take advantage of the single ion contributions, especially by incorporating into the cluster a diamagnetic divalent 3d cation using compartmental ligands,15 which is one of the best ways to control the number and nature of metal ions in the same molecule. There is a wide variety of ligands, which allows the binucleation by using sets of different donor atoms. The hexadentate Schiff base N,N′-ethylenebis(3-ethoxysalicylaldiimine) is a popular ligand (more than 300 entries in the CCDC) by several reasons like its easy syntheses by the condensation of ethylenediamine and o-vanillin and its compartmental structure, with two well differentiated cavities, which allows easy and reproducible syntheses: the O2O′2 compartment can easily accommodate the large oxophilic lanthanide and the inner and smaller N2O2 pocket hosts adequately the 3d cation. Moreover, parallel syntheses starting from substituted diamines with chiral centres (cyclohexanediamine, 1,2-propanediamine or 1,2-diphenyl-ethylenediamine) become an interesting route for the synthesis of chiral ligands potentially useful for enantioselective catalysis or for introducing optical properties into the clusters. The most usual synthesis of these types of complexes is a two-step reaction that consists of the formation of a mononuclear complex with the ligand and the 3d cation followed by the reaction of the mononuclear precursor with the lanthanide salt. The diamagnetic ZnII cation has been the preferred 3d ion with these kinds of ligands to promote a magnetic dilution because when the 3d metal is diamagnetic, the larger size of the dinuclear compounds can diminish the

intermolecular interactions, mainly the dipolar ones.16 This technique has been used with ZnII/LnIII clusters showing different topologies and nuclearities, the vast majority of them being trinuclear ZnII···DyIII···ZnII systems17a–d and in some other few cases other LnIII cations,17a,b,e,f allowing a good isolation between LnIII cations and SIM response, while the dinuclear systems have been studied exclusively for the [ZnIIDyIII] and [ZnIITbIII] cases.18 On the other hand, it has also been demonstrated recently that the diamagnetic ZnII can influence the electronic density distribution of the coordinating ligands around the lanthanide cation19 (mainly for the bridging O-donors), influencing the SMM response and specially the direction of the g tensor of the lanthanide by modifying its environment.20 However, the drawback of this magnetic dilution method is that in the case of salen-type ligands the coordination of ZnII is square pyramidal, with the four basal sites occupied by the Schiff base and one axial site linking anions or solvent molecules favouring the presence of hydrogen bonds between molecules and reducing the effective magnetic isolation. For this reason, we decided to try a better magnetic dilution for [MIILnIII] systems with salen-type Schiff bases to try and reduce the intermolecular interactions by replacing the ZnII cation with usually five coordination positions with the NiII cation, which prefers the square-planar coordination with these kinds of ligands and avoids the undesired intermolecular H-bonds. Even the core with diamagnetic NiII and this kind of Schiff base has been prepared before, and dynamic magnetic measurements have been reported only in one case21 for Ln = DyIII and TbIII.

In general terms, magnetic dilution has been tried with ZnII, MgII, CaII, AlIII, low-spin CoIII or square-planar NiII, the latter being less studied.19a

On the basis of the above considerations and to explore the dynamic magnetic properties of the [MIILnIII] core for the f-series with the two diamagnetic ZnII and NiII cations, we decided to design chiral heterometallic [MIILnIII] systems using the mentioned two step sequential reaction of an enantiomerically pure H2L Schiff base (Scheme 1) with NiII or ZnII followed by the binucleation with the lanthanide.

The procedure allowed the characterization of two series of [NiIILnIIIL(NO3)3] neutral complexes where LnIII = Eu (1RR, 1SS), Ce (3RR), Nd (4RR), Dy (5RR), Er (6SS) and Yb (7SS) and [ZnIILnIIIL(MeOH)(NO3)3]·MeOH dimers where LnIII = Eu (2RR, 2SS), Ce (8RR), Nd (9RR), Dy (10SS), Er (11SS) and Yb (12RR). Single crystal X-ray diffraction demonstrates that the ZnII family of complexes suffers a two-step loss of solvents, yielding the intermediate [ZnIIEuIIIL(MeOH)(NO3)3]·1/2MeOH (2RRb) and a further loss of the coordinated methanol and the incorporation of two water molecules [ZnIILnIIIL(H2O)(NO3)3]·H2O (2RRc). The new complexes have been characterized by ECD spectroscopy and susceptibility measurements which revealed slow relaxation of magnetization under an applied external magnetic field in the two series for the oblate CeIII, NdIII and DyIII complexes whereas the prolate ErIII and YbIII show only clear out-of-phase

112 signals for the [NiIIILnIII] core, suggesting that the NiII diamagnetic cation promotes a most efficient
113 magnetic dilution by reducing the intermolecular interactions.

114

EXPERIMENTAL

X-ray crystallography

Prismatic crystals of 1RR, 1SS, 2RR and 2SS were used for single crystal X-ray crystallographic analysis. 2SSb and 2SSc were measured on the same crystal after exposure of 2SS in open air for 48 h and one week, respectively. The X-ray intensity data were measured on a D8 Venture system equipped with a multilayer monochromator and a Mo microfocus ($\lambda = 0.71073$ Å). The frames were integrated with the Bruker SAINT software package using a narrow-frame algorithm. Data were corrected for absorption effects using the multi-scan method (SADABS). The structures were solved and refined using the Bruker SHELXTL Software package. Unit cell parameters and structure solution and refinement data for the six structures are listed in Tables S1 and S2.† Further crystallographic details can be found in the corresponding CIF files provided in the ESI.†

Powder X-ray diffraction was performed with a PANalytical X'Pert PRO MPD θ/θ powder diffractometer of 240 millimetres of radius, in a configuration of convergent beam with a focalizing mirror and a transmission geometry with flat samples sandwiched between low absorbing films and using Cu Kα radiation ($\lambda = 1.5418$ Å). Comparison between the calculated spectrum from the single crystal structure of the enantiomers of compounds 1 and the experimental spectra for the whole series of powdered [NiIILnIII] samples 3–7 gives a perfect match which confirms the isostructurality among them, Fig. 1.

The powdered samples of the series of complexes [ZnIILnIII] 8–12 revealed to be also isostructural among them but, surprisingly, their spectra were completely different from the calculated spectrum from single crystal diffraction of 2RR/2SS, Fig. 2.

To check if the problem was due to the loss of solvent molecules, a new crystal of 2SS was measured immediately after extraction of the mother liquor and after checking that the structure was the same, another single crystal measurement was made after 48 h of exposure to open air. The new structure (2SSb) shows a partial loss of one half of the crystallization methanol molecules but the simulated powder spectra were quite similar to that of 2SS, Fig. 2. This brought us to do a third collection of data after one week of exposure to open air and the resulting structure (2SSc) revealed the complete removal of the crystallization solvent and also that the coordinated methanol molecules were substituted by water from the ambient moisture. The calculated powder spectra agreed with those obtained from the powdered samples employed for instrumental measurements, Fig. 2. From these data, the last structure (2SSc) and its corresponding molecular weight must be assumed as the most adequate to analyse further measurements.

Physical measurements

Magnetic susceptibility measurements were carried out on polycrystalline samples with a MPMS5 Quantum Design susceptometer working in the range 30–300 K under magnetic fields of 0.3 T and under a field of 0.03 T in the 30–2 K range to avoid saturation effects at low temperature. Diamagnetic corrections were estimated from Pascal tables. Infrared spectra (4000–400 cm−1) were recorded from KBr pellets on a Bruker IFS-125 FT-IR spectrophotometer. ECD spectra were recorded in dichloromethane or methanolic solutions in a Jasco-815 spectropolarimeter. Solid-state fluorescence spectra were recorded with a Horiba Jobin Yvon SPEX Nanolog fluorescence spectrophotometer at room temperature.

RESULTS AND DISCUSSION

Syntheses

Choice of complexes. One cation of intermediate size (EuIII) was selected to obtain the X-ray single crystal structures. The remaining complexes characterized by powder X-ray diffraction were shown to be isostructural and thus, the full resolution of the remaining structures was not necessary for the purpose of this work. For the selected EuIII complexes both enantiomers were synthesized and structurally characterized whereas for the other cations only one enantiomer was synthesized to check their emissive properties. Magnetic measurements were performed for one of the enantiomers because they must give identical response. Following the same experimental procedure the PrIII, SmIII, TbIII, HoIII and TmIII derivatives were also prepared but they do not give any spectroscopic (VIS or NIR luminescence) or out-of-phase magnetic response (for the non-Kramer cations TbIII, HoIII and TmIII). Therefore their details have not been included in the list of reported complexes.

H2L ligand. A solution of 0.304 g (2 mmol) of o-vanillin and 0.212 g (1 mmol) of (RR) or (SS)-1,2-diphenyl ethylenediamine in 10 mL of methanol was refluxed for six hours. The resulting solution of the Schiff base was diluted to a volume of 40 Ml and employed directly to synthesize the derived complexes without the isolation of the solid ligand. Similar syntheses were previously reported.17,18

[NiLn(L)(NO3)3]. The syntheses are common for all the lanthanide complexes 1–7. 0.062 g (0.25 mmol) of nickel acetate tetrahydrate were dissolved in a minimum amount of methanol, and to this solution was added 10 mL (0.25 mmol) of the previously prepared solution of H2L. The resulting dark orange solution was refluxed for 1 hour. To this solution 0.25 mmol of the corresponding lanthanide nitrate n-hydrate salt was added in solid. After the dissolution of the lanthanide salt, the colour changes to light orange and, after some minutes, a red powder of the corresponding complex starts to precipitate. Well-formed orange crystals for X-ray diffraction of the europium complex were obtained after few days by vapour diffusion with diethyl ether. Relevant IR bands: 3057 (w), 1613 (s) characteristic –CvN– stretching band, 1559 (w), 1472 (s), 1384 (m) (evidencing the presence of nitrates), 1314 (s), 1276 (s), 1234 (s), 1200 (w), 1173 (w), 956 (w), 864 (w), 813 (w), 781 (w), 740 (m), 696 (m), 506 (w).

[ZnLn(L)(MeOH)(NO3)3]·MeOH. The syntheses were common for all the lanthanide complexes 2, 8–12. 0.074 g (0.25 mmol) of zinc nitrate were dissolved in a minimum amount of methanol and added to 10 mL (0.25 mmol) of the previously prepared solution of H2L and the resulting yellow solution was refluxed for 1 hour. 0.25 mmol of the corresponding hydrated lanthanide nitrate were added in solid. Wellformed yellow crystals for X-ray diffraction of the 2RR and 2SS complexes were obtained by vapour diffusion with diethyl ether. The solubility of some of the [ZnIILnIII] complexes is slightly different from that of the [NiIILnIII] systems, and they only crystallize by vapour diffusion when the solutions were previously reduced to one third of their original volume under reduced pressure. IR spectra are similar to those of the NiII complexes, showing the characteristic set of weak C–H bands at

3058/3030/2955/2853 cm−1, the CvN stretching varying from 1610 to 1630 cm−1 for the whole series of compounds and the N–O stretching of the nitrate at 1384 cm−1. See Fig. S1† for representative spectra of each series.

A faster synthesis can be performed by heating a methanolic solution of o-vanillin and 1,2-diphenyl ethylenediamine at 80° in a microwave furnace, followed by ten minutes at the same temperature after the addition of the 3d salt and ten additional minutes at the same temperature after the addition of the lanthanide salt.

Description of the structures

The mirror-image structures of the pairs of the enantiomeric [NiIIEuIII] 1RR/1SS and [ZnIIEuIII] 2RR/2SS complexes contain two non-equivalent A/B molecules in the unit cell with minor differences in the bond parameters. To avoid repetitive text the following description will be referred to as the A-molecule of one of the enantiomers, assuming that there are minimal differences with respect to the corresponding B-molecule or with respect to the other enantiomers. [NiEu(L)(NO3)3] (1). A partially labelled plot of 1RR is shown in Fig. 3 and selected bond parameters are summarized in Table 1. The representative structure of 1RR consists of neutral

[NiIIEuIII] dinuclear complexes in which the NiII cation is coordinated to the inner N2O2 pocket of the Schiff base while the most hard EuIII cation is coordinated to the external phenoxo/methoxy O2O′2 donors. The NiII cation is tetracoordinated (square planar) with Ni–N/Ni–O distances in the short 1.806–1.843 Å range and N–Ni–O bond angles larger than N–Ni–N and O–Ni–O angles (∼95° vs. ∼85°), whereas the EuIII cation completes its coordination sphere with three bidentate nitrato ligands, with the EuIII–O(nitrate) distance being slightly larger than EuIII–O(phenoxo) and EuIII–O(methoxy) distances. SHAPE22 calculations indicate that the coordination polyhedron around the EuIII cation is close to an ideal sphenocorona (C2v, CShM = 3.24, Table S3†), distorted due to the low bite angle of the bidentate nitrato ligands, Fig. 3.

The NiII-Schiff base fragment is essentially planar. The dihedral angle between the mean [NiN2O2] molecular plane and the plane defined by O2/O3/Eu1 is 15.9° and consequently the EuIII ion is displaced by 0.56 Å out of the [NiN2O2] plane.

The molecules are well isolated and in addition to weak C– H···O H-bonds the only intermolecular interactions consist of CH–π(ring) contacts, Fig. 4. This kind of supramolecular interaction between aromatic rings acting as H-bond acceptors and –CH groups as H-donors plays an important role in biological systems and is often determinant in the crystal packing of molecular compounds.23 In this case, the interaction is established between one H-atom of one of the methyl groups of the L2− ligands which is directed towards the centroid of one phenyl group of the neighbouring molecule.

Noteworthily, this interaction generates chains of strictly A or B molecules. The distance between H30B and the centroid of the phenyl ring C17A/C22A is 2.644 Å with a C30A–H30B···centroid angle of 148.9°. The non-equivalent B molecules show similar parameters, 2.596 Å being the distance between H1BC and the centroid of the phenyl ring C17B/C22B and 163.3° being the C30A–H30B···centroid angle.

[ZnEu(L)(MeOH)(NO3)3]·MeOH (2RR/2SS·MeOH). As in the above described [NiIIEuIII] complexes, the structures of the enantiomers 2RR and 2SS contain two similar but non-equivalent dimers in the unit cell (labelled A/B) and the description will also be centered on the 2SS(A) molecule. The ZnII cation is pentacoordinated with a square pyramidal environment, which is defined by the N2O2 donors of the Schiff base and one methanol molecule in the apical coordination site, Fig. 5. Main bond parameters are summarized in Table 2. As a consequence of this coordination, the ZnII ion is placed 0.540 Å out of the plane defined by the N2O2 atoms. Bond distances are slightly larger than that for the NiII case, ranging between 1.984–2.047 Å. The EuIII cation is coordinated to two O-phenoxo donors that act as a bridge with the ZnII cation, two O-methoxy donors and three bidentate nitrate ligands. The O2/O3/Eu1 plane and the mean plane defined by the base of the coordination polyhedron of the ZnII cation (N2O2 plane) dihedral angle is 23.6° and the EuIII cation is placed 0.77 Å out of the main molecular plane. The presence of methanol molecules in the structure generates a set of hydrogen bonds between the coordinated methanol, the crystallization solvent and one nitrate of the neighbouring molecule and leads to the formation of one-dimensional zigzag AB chains running parallel to the crystallographic c axis, as is shown in Fig. 5. Interactions between chains consist of CH–π(ring) interactions established between two H-atoms of the methyl groups of the coordinated methanol and the phenyl rings of the neighbouring molecule, with the distance to the centroids of the rings of 3.025 and 3.275 Å (Fig. S2†).

[ZnEu(L)(MeOH)(NO3)3]·1/2MeOH (2SSb·0.5MeOH). The structure of complex 2SS·MeOH after exposure to open air for 48 h is practically equal to that of 2SS at the molecular level. The ZnII and EuIII environments are very close to the above described and the changes in the bond parameters are minimal. The structure is shown in Fig. S3† and the bond parameters are summarized in Table S4.† The main difference between 2SSb and 2SS consists of the loss of one half of the crystallization methanol molecules involved in the intramolecular H-bonds that determine the 1-D arrangement of dimers. In this case one of the interactions remains as that in 2SS but the partial loss of solvent promotes the direct H-bond between the methanol molecule coordinated to the ZnII cation with one nitrate anion coordinated to the neighbouring molecule, resulting in a chain of dimers, alternatively linked by the two kinds of H-bonds, Fig. 6.

[ZnEu(L)(H2O)(NO3)3]·H2O (2SSc·H2O). The structure of 2SSn after air exposure for one week shows a similar dinuclear molecular structure but with different environments around the ZnII cation, which in this case shows a water molecule coordinated in the apical position of its square pyramidal

environment. A labelled plot of the structure is depicted in Fig. 7 and main bond parameters are summarized in Table 3. The ZnII cation is placed 0.53 Å over the N2O2 base of the square pyramid and the EuIII cation 0.60 Å over this plane. All the crystallization methanol molecules are lost and a crystallization water molecule has been incorporated into the structure. The crystallization water molecule forms two strong intramolecular H-bonds with the coordinated water and one O-atom from one of the nitrates with O14···O1W and O12···O1W distances of 2.66(2) and 2.62(2) Å respectively. The dinuclear entities are in this case linked in a regular fashion by H-bonds between the coordinated water molecule and one O-atom of one of the nitrates of the neighbouring molecule, Fig. 7, forming a chain of dinuclear complexes linked by H-bonds that runs along the c crystallographic axis.

SHAPE22 calculations indicate that the coordination polyhedron around the EuIII cation is closer in this case to an ideal tetradecahedron (TD-10) (C2v, CShM = 2.78, Table S3†), distorted due to the low bite angle of the bidentate nitrato ligands, Fig. 7.

Comparison with the structure of complexes 1 evidences a key point for further magnetic studies: the substitution of ZnII by NiII is far from innocent because it induces changes in the planarity and conformation of the ligand, on the coordination sphere of the lanthanide and mainly, in the intermolecular interactions.

Ligand conformation. For the chiral (R,R/S,S) ligands there are two conformational possibilities related to the relative position of the phenyl rings, that can be placed on the main molecular plane or perpendicular to this plane, as it occurs for the [ZnIIEuIII] and [NiIIEuIII] complexes, Fig. 8. The in-plane conformation seems to be the most usual and has been observed in several mononuclear complexes containing VOII, octahedral VIV or dinuclear CuIIGdIII or ZnIIDyIII dimers18c,24 whereas the perpendicular arrangement of the phenyl groups has only been observed in one case for NiII.25 This difference does not come from the crystallization process of the dinuclear complex and must be related to the formation of the NiL or ZnL precursor because the free rotation around the C–C bond is only possible while the ligand remains in solution until it reacts with the corresponding cation and adopts a fixed conformation.

Chirality transfer and electronic circular dichroism

Transference of chirality from the chiral ligand to the metallic centres is poor in this case because in spite that the coordination polyhedra around the cations show a mirror image between the RR and SS complexes, there are minimal differences in square planar (NiII) or square pyramidal (ZnII) environments. Similarly the differences around the lanthanide cation are small and limited to the relative torsion of the nitrato groups and thus, the chiroptical properties must be mainly related to the ligands. Electronic circular dichroism (ECD) spectra in dichloromethane or methanolic solution were recorded

for the representative enantiomeric pairs of 1 and 2 respectively. The spectra of 1 show the same bands as 2 but shifted by 25 nm to higher wavelengths and with different intensities that must be attributed to the different conformations of the phenyl rings shown in Fig. 8. The representative ECD spectra for the pairs of complexes 1RR/1SS and 2RR/2SS are shown in Fig. 9 and their mirror image confirms the enantiomeric nature of the reported complexes. The spectrum of the NiIIEuIII complexes was poor due to the low solubility of the complexes but exhibited a positive Cotton effect at λmax =410, 370(sh) and 290 nm and a negative band at 325 nm for 1RR and the bands with opposite signs for 1SS. The spectrum of the ZnIIEuIII complex 2RR shows a positive Cotton effect at 218, 265, 342 and 395 nm a weak negative band at 235 and an intense absorption at 300 nm for 2RR and a mirror image for 2SS.

Luminescence measurements. The ZnII complexes with Schiff bases are good antenna to transfer energy to the LnIII cations and often the [ZnIILnIIIZnII] or [ZnIILnIII] related systems have shown luminescence.17,18

The emissive properties of the reported complexes and the [NiL] and [ZnL] precursors were checked in the NIR and in the visible region. Unfortunately, only the [ZnL] mononuclear complex exhibits a typical green luminescence with an emission band centred at 489 nm under excitation at 380 nm, Fig. S4,† whereas for the dinuclear complexes the LnIII emission was completely quenched.

Magnetic measurements

The magnetic susceptibility for complexes 3–7 and 8–12 in the form of χMT product vs. temperature performed on polycrystalline samples in the 2–300 K range is shown in Fig. S5.† χMT values at room temperature are close to the expected values for the corresponding isolated lanthanide cations 2F5/2 (CeIII, 0.80 cm3 mol−1 K), 4I9/2 (NdIII, 1.60 cm3 mol−1 K), 7F6 (TbIII, 11.82 cm3 mol−1 K), 6H15/2 (DyIII, 14.17 cm3 mol−1 K), 4I15/2 (ErIII, 11.48 cm3 mol−1 K) and 2F7/2 (YbIII, 2.57 cm3 mol−1 K), and are in agreement with the null contribution of the S = 0 square planar NiII or square pyramidal ZnII cations. In all cases the χMT product remains almost constant until the temperature reaches 150 K, where the values start to steadily decrease for complexes 3–7 and 8–12, due to the progressive depopulation of the MJ states and, at low temperature, the possibility of weak antiferromagnetic interactions between molecules, tending to finite values.26 Theoretically, the EuIII analogues, 1 and 2, should not exhibit any magnetic moment because EuIII has 7F0 (J = 0), although some contribution from thermally accessible levels appears as usual at high temperature, and χMT tends to zero at low T.

Recently Lloret et al.27 reported a series of lanthanide-containing complexes with an ideal D3h symmetry (trigonal axial symmetry) where the magnetic properties can be simplified supposing implicitly a regular distribution of the MJ states using the Hamiltonian:

$$H = \lambda LS + \Delta[L_z^2 - L(L+1)/3] + \beta H(-kL + 2S)$$

in which the first term describes the spin–orbit coupling, the second one is about the axial ligand field component and the third one is the Zeeman effect, parameterized with the spin–orbit coupling parameter λ, the gap between ML components, Δ and the orbital reduction parameter, k. To check if the above Hamiltonian is able to reproduce the experimental data in lower symmetries giving information of the ground MJ state, we implemented it in the PHI program.28 This Hamiltonian is not accurate enough in low symmetry but the χMT simulations were surprisingly good for most of the complexes, Fig. S5 and S6.†

In order to study the dynamic magnetic properties, temperature and frequency variable ac measurements were performed on polycrystalline samples of all the compounds. No maxima appear in the χ″M vs. T measurements above 1.8 K for any of the [NiIIILnIII] or [ZnIIILnIII] compounds indicating that the magnetic moments completely follow the magnetic field due to the fast reversal of magnetization through QTM inbetween the low lying ground state doublets. For this reason, we decided to explore the effect of an external dc field on the relaxation processes trying to avoid the QTM, typical of lanthanide magnetic molecules in distorted environments. The preliminary measurements were performed scanning at 10 Hz and 1000 Hz frequencies under different dc fields between 500 and 2000 G and selecting the field that induces the clearest signal, Fig. S7.† In light of these measurements fields of 500 G were selected for 3 and 8, 2000 G for 12 and 1000 G for the remaining compounds. Under the indicated fields, clear dependence of the out-of-phase signal vs. frequency and temperature was found for the two series of complexes for the cations CeIII (3, 8), NdIII (4, 9), DyIII (5, 10) and only for the ErIII (6) and YbIII (7) derivatives for the [NiIIILnIII] series (Fig. 10 and S8–9†), evidencing the suppression of the fast relaxation path in Kramers doublets. Only very weak tails for the ErIII (11) and YbIII (12) [ZnIIILnIII] complexes were observed. Since the discovery of the slow relaxation of magnetization in coordination compounds,29 the magnetic memory has been attributed to complexes with a negative anisotropy like 5 and 12, due to the presence of energy barriers separating states with opposite spin orientations along the anisotropy axis. However, complexes 3, 4, 6–9, 11 and 12 present slow relaxation of magnetization under an applied dc field even if their ground state has a major contribution of the lower MJ value as has been previously observed.27 The fact that a cluster with a positive anisotropy value can behave as a single molecule magnet was demonstrated some time ago by Long and co-workers under an external dc field.30 At this point, two different approaches, that require different treatments of the data, were used for the calculation of the magnetic relaxation parameters of the systems, Table 4: first kinds of compounds show peaks above 2 K in the frequency range 10–1488 Hz. In these cases, an Arrhenius dependency fitting was used to calculate the relaxation time (τ0) and relaxation barrier (Ueff) (Fig. S10†), by means of the equation:

$$\ln(1/(2\pi\omega)) = \ln(1/\tau_0) - U_{eff}/(k_B T))$$

which supposes the so-called Orbach relaxation,31 which is produced at relatively high temperature by means of involving two phonons in a spin–lattice relaxation, involving relaxation through real states. Other compounds do not show maxima in the $\chi''M$ vs. temperature representations, but there is a clear dependence of $\chi''M$ with temperature. In these cases, the sonamed generalized Debye model was employed (Fig. S10†), to find the relaxation parameters according to the expression:32

$$\ln(\chi''_M/\chi'_M) = \ln(\omega\tau_0) - U_{eff}/(k_B T).$$

It is important to mention that complexes 3, 4, 7, 8 and 9 join the scarce number of molecules with slow relaxation of magnetization prepared with lanthanides known as "uncommon magnetic lanthanides".10,33,34

In the last few years, hundreds of articles have appeared on lanthanide clusters presenting slow relaxation of magnetization, the vast majority of them with TbIII and DyIII cations, DyIII being the most popular by far due to its high magnetic moment and its Kramers ion condition, which make it a very good candidate for achieving SMM/SIM behaviour.

However, all lanthanides can present SMM behaviour in an appropriate environment by a proper design of the ligand field14,33,34 by differentiating the oblate or prolate character of the different lanthanide(III) cations. Among the uncommon lanthanides, CeIII is a desirable cation to work17b because it does not present nuclear spin and makes zero field QTM less efficient. Even CeIII has only one electron in the 4f shell (4f 1, 2F5/2) and has a strong enough spin–orbit coupling to allow magnetic anisotropy. Ac susceptibility measurements were carried out for complexes 3 and 8, and, as was mentioned before, no signature of slow relaxations was found under a zero applied field. This is due to the fact that in these compounds Δ is positive, with the Stark doublet MJ = ±1/2 probably being the low-lying level which promotes significant QTM.34 Even a positive Δ supposes no barrier and the spin is free to rotate, and an anisotropy easy plane is derived from the very low symmetry.

The same reasoning can be used for NdIII analogues. Their electronic configuration (4f 3, 4I9/2) allows enough spin–orbit coupling to permit the needed anisotropy for a slow relaxation of magnetization and the positive Δ of compounds 4 and 9 does not allow relaxation under a zero dc field. To end with the uncommon lanthanides, only the NiII derivative with YbIII (7) presents slow relaxation of magnetization under an external magnetic field strong enough to quench the quantum tunnelling of magnetization (Fig. 10 and S8–9†). Although YbIII is highly anisotropic, there is a scarce number of SMM reported,35 and is by far the most popular of the "uncommon lanthanides". We calculated a positive Δ value for the YbIII derivatives, so again, the ground state should be MJ = ±1/2. However, the YbIII complexes with slow relaxation of magnetization under a dc external field reported in the literature support in most of the cases a MJ = ±5/2 as the ground doublet10 calculated by means of the

Stevens operators, ac data and luminescence spectra, and all of them present higher symmetry conditions. That is why in our low symmetry environment, we can support a mix of the MJ states.

Turning now to the most common lanthanides, DyIII and ErIII, they did not present any signs of slow relaxation of magnetization under a zero dc field. For complexes 5, 6, 10 and 11, evidence of induced SIM behaviour was only observed for 5, 6 and 10. The DyIII (4f 9, 6H15/2) derivatives 5 and 10 showed a Δ negative value, so we can assume that the higher MJ state is the ground one, with probably mixing with the low lying excited states due to the low symmetry, but allowing a large enough barrier to the relaxation. For the ErIII derivatives (4f 11, 4I15/2), with positive Δ, only the compound 6 from the NiII family presents slow relaxation of magnetization.

The calculated values of the energy barriers for all the compounds, Table 4, are by far too low than the first excited state for any LnIII cation and so, an over barrier relaxation is not allowed. This is a usual discrepancy in the f-element magnetic molecules, and is attributed to dipolar interactions between paramagnetic canters and a mixing of the low lying excited states.

Due to the low symmetry environment around the lanthanide cations and due to the fact that all of them present fast relaxation of magnetization under a zero dc field, in all of the here reported complexes we assume a mixing of the low lying excited states, independent of the sign of Δ as a direct consequence of the low environment symmetry. Cole–Cole36 plots of 3–9 (Fig. S11 and S12†) were fitted using CCfit software and the generalized Debye model:37

$$\chi(\omega) = \chi_S + (\chi_T + \chi_S)/(1 + i\omega\tau)^{1-\alpha}$$

where χS and χT are the adiabatic and thermal susceptibilities respectively, τ is the average relaxation time and α is a parameter ranging from 0 to 1 which quantifies the width of the relaxation time distribution. For all of them, the Cole–Cole plots result in only one semicircle supposing a single relaxation process for each complex yielding an α value lower than 0.3 for all of them, with a narrow distribution of the relaxation time. For complexes 3–9, the representation of τ0 −1 vs. T shows that for all of them, the relaxation rate decreases with decreasing temperature, but no unique exponential law can simulate this dependence in all the temperature ranges evidencing that the Orbach relaxation may be mixed with a faster relaxation process. However, in the representation of ln(τ0) vs. the inverse of the temperature (Fig. S13,† inset), there is no evidence of a temperature-independent plateau at low temperatures, indicating that the relaxation process is still dependent on temperature, so QTM as a secondary relaxation path must be excluded above 2 K, the minimum temperature allowed by the instrument. Even if the fit parameters are poorly reliable in absolute terms,38 the plots have been fitted following a Raman and Arrhenius dependence, Fig. S13.†

Complexes 3–10 have an Arrhenius dependency of the relaxation time with temperature (Fig. S13†), but at the same time, the relaxation barrier calculated by means of this dependency is too low to overcome

437 the anisotropy barrier. Below 3 K, no maxima appears in the χ″M vs. temperature plots for the vast
438 majority of complexes and the linear dependency between τ0 and T disappears, meaning that below this
439 temperature relaxation between Kramers states cannot be supposed as Orbachlike relaxation, but some
440 kind of temperature dependency remains. For this reason, we suppose that there is a non-complete van
441 Vleck cancellation, and Raman relaxation is active due to intermolecular interactions.39

442 Complex 10 shows a slightly different behaviour in the relaxation features, as can be seen clearly in the
443 representation of χ″ vs. temperature in Fig. S9,† where one maximum and a shoulder appear. The
444 apparition of two processes is usually attributed to two crystallographically independent DyIII cations in
445 the unit cell. However, the quasi identical environment and consequently, the crystal field around the
446 cations do not support this hypothesis in this case. This feature for DyIII has been reported in numerous
447 cases40 and the low temperature processes have been attributed to direct relaxation under a dc
448 field.19,41

449 Summarizing the above results, there are several experimental features that deserve a final comment. (1)
450 These systems have strong QTM and the barriers of reversal of magnetization are low in all cases and
451 comparable to the few bibliographic examples (only DyIII and TbIII) with similar ligands. This fact
452 must be attributed to the low symmetry of the coordination polyhedron around the LnIII cations. (2)
453 Interestingly, the oblate ions CeIII, NdIII and DyIII do not show a significant difference in behaviour
454 when ZnII is replaced with NiII, all of them presenting similar response and values of the relaxation
455 parameters, suggesting that the change of the diamagnetic cation does not promote differences in the
456 ligand field of these lanthanides. In contrast, the prolate cations ErIII and YbIII clearly show better
457 response for the [NiIILnIII] family. It has been proved that the diamagnetic cation can modify the
458 electronic density and the field promoted by the μ-O bridges19 and in our case, the prolate cations must
459 be more sensitive to changes in the environment due to the distribution of the field around the lanthanide
460 cation: the O-donors with negative charge are roughly placed in a plane with the neutral ones placed
461 axially, Fig. 11. Better isolation of the dimers and the change of the diamagnetic cation suggest that in
462 this case different responses for oblate/prolate lanthanides are promoted.

463

CONCLUSIONS

This paper presents the structure and the optical and magnetic characterization of 14 new complexes belonging to two different series of [MIILnIII] dimers (M = NiII, ZnII). Single crystal X-ray diffraction evidences that the employment of the square planar NiII cation as a diamagnetic 3d ion is a better option than the pentacoordinate ZnII cation in order to avoid intermolecular H-bonds or structural changes due to the labile ZnII–solvent bonds. The characterization of five new induced SIMs with the unusual lanthanide cations CeIII, NdIII and YbIII is remarkable. A general conclusion can be made that the better isolation of the Ni family due to the lack of hydrogen bonds between molecules and the experimental better response of the prolate cations, while there is no significance

ACKNOWLEDGEMENTS

Funds from Ministerio de Economia y Competitividad, Project CTQ2015-63614-P are acknowledged.

NOTES AND REFERENCES

X. Yang, S. Wang, T. King, C. J. Kerr, C. Blanchet, D. Svergun, R. Pal, A. Beeby, J. Vadivelu, K. A. Brown, R. A. Jones, L. Zhang and S. Huang, Faraday Discuss., 2016, 191, 465.

D. T. Thielemann, A. T. Wagner, E. Roesch, D. K. Koelmel, J. G. Heck, B. Rudat, M. Neumaier, C. Feldmann, U. Schepers, S. Brase and P. W. Roesky, J. Am. Chem. Soc., 2013, 135, 7454.

(a) G. Xiao, B. Yan, R. Ma, W.-J. Jin, X.-Q. Lu, L.-Q. Ding, C. Zeng, L.-L. Chen and F. Bao, Polym. Chem., 2011, 2, 659; (b) W.-J. Jin, L.-Q. Ding, Z. Chu, L.-L. Chen, X.-Q. Lu, X.-Y. Zheng, J.-R. Song and D.-D. Fan, J. Mol. Catal. A: Chem., 2011, 337, 25; (c) O. V. Amirkhanov, O. V. Moroz, K. O. Znovjyak, T. Y. Sliva, L. V. Penkova, T. Yushchenko, L. Szyrwiel, I. S. Konovalova, V. V. Dyakonenko, O. V. Shishkin and V. M. Amirkhanov, Eur. J. Inorg. Chem., 2014, 3720.

Y.-Z. Zheng, E. M. Pineda, M. Helliwell and R. E. P. Winpenny, Chem. – Eur. J., 2012, 18, 4161.

(a) K.-Y. Zhang, Q. Yu, H. Wei, S. Liu, Q. Zhao and W. Huang, Chem. Rev., 2018, 118, 1770; (b) F. Zinna and L. Di Bari, Chirality, 2015, 27, 1.

S. I. Weissman, J. Chem. Phys., 1942, 10, 214. 7 F. Habib and M. Murugesu, Chem. Soc. Rev., 2013, 42, 3278.

J. D. Rinehart, M. Fang, W. J. Evans and J. R. Long, Nat. Chem., 2011, 3, 538.

H. L. C. Feltham and S. Brooker, Coord. Chem. Rev., 2014, 276, 1.

F. Pointillart, O. Cador, B. Le Guennic and L. Ouahab, Coord. Chem. Rev., 2017, 346, 150.

(a) Y. Lan, S. Klyatskaya and M. Ruben, Lanthanides and Actinides in Molecular Magnetism, Wiley-WCH, Weinheim, 2015, p. 223; (b) M. N. Leuenberger and D. Loss, Nature, 2001, 410, 789; (c) F. Troiani and M. Affronte, Chem. Soc. Rev., 2011, 40, 3119.

(a) K. S. Pedersen, A. M. Ariciu, S. McAdams, H. Weihe, J. Bendix, F. Tuna and S. Piligkos, J. Am. Chem. Soc., 2016, 138, 5801; (b) D. N. Woodruff, R. E. P. Winpenny and R. A. Layfield, Chem. Rev., 2013, 113, 5110.

N. Ishikawa, M. Sugita, T. Ishikawa, S. Y. Koshihara and Y. Kaizu, J. Am. Chem. Soc., 2003, 125, 8694.

(a) J. D. Rinehart and J. Long, Chem. Sci., 2011, 2, 2078; (b) J.-L. Liu, Y.-C. Chen and M.-L. Tong, Chem. Soc. Rev., 2018, 47, 2431.

507 (a) M. Andruh, Dalton Trans., 2015, 44, 16633; (b) M. Andruh, Chem. Commun., 2011, 47, 3025.

508 (a) A. Caneschi, L. Sorace, U. Casellato, P. Tomasin and P. A. Vigato, Eur. J. Inorg. Chem., 2004, 3887;
509 (b) T. D. Pasatoiu, C. Tiseanu, A. M. Madalan, B. Jurca, C. Duhayon, J. P. Sutter and M. Andruh,
510 Inorg. Chem., 2011, 50, 5879; (c) V. Bereau, H. Bolvin, C. Duhayon and J. P. Sutter, Eur. J.
511 Inorg. Chem., 2016, 4988; (d) K. Griffiths, J. Mayans, M. A. Shipman, G. J. Tizzard, S. J. Coles,
512 B. A. Blight, A. Escuer and G. E. Kostakis, Cryst. Growth Des., 2017, 17, 1524; (e) M. Fondo, J.
513 Corredoira-Vazquez, A. M. Garcia-Deibe, J. Sanmartin-Matalobos, J. M. Herrera and E. Colacio,
514 Inorg. Chem., 2017, 56, 5646.

515 (a) M. Maeda, S. Hino, K. Yamashita, Y. Kataoka, M. Nakano, T. Yamamura and T. Kajiwara, Dalton
516 Trans., 2012, 41, 13640; (b) P.-L. Then, C. Takehara, Y. Kataoka, M. Nakano, T. Yamamura and
517 T. Kajiwara, Dalton Trans., 2015, 44, 18038; (c) W.-B. Sun, P.-F. Yan, S.-D. Jiang, B.-W. Wang,
518 Y.-Q. Zhang, H.-F. Li, P. Chen, Z.-M. Wang and S. Gao, Chem. Sci., 2016, 7, 684; (d) A. L.
519 Boulkedid, J. Long, C. Beghidja, Y. Guari, A. Beghidja and J. Larionova, Dalton Trans., 2018,
520 47, 1402; (e) S. Hino, M. Maeda, Y. Kataoka, M. Nakano, T. Yamamura and T. Kajiwara, Chem.
521 Lett., 2013, 42, 1276; (f) C. Takehara, P.-L. Then, Y. Kataoka, M. Nakano, T. Yamamura and T.
522 Kajiwara, Dalton Trans., 2015, 44, 18276.

523 (a) J. Long, R. Vallat, R. A. S. Ferreira, L. D. Carlos, F. A. Almeida Paz, Y. Guari and J. Larionova,
524 Chem. Commun., 2012, 48, 9974; (b) P. Zhang, L. Zhang, S.-Y. Lin and J. Tang, Inorg. Chem.,
525 2013, 52, 6595; (c) J. Long, J. Rouquette, J. M. Thibaud, R. A. S. Ferreira, L. D. Carlos, B.
526 Donnadieu, V. Vieru, L. F. Chibotaru, L. Konczewicz, J. Haines, Y. Guari and J. Larionova,
527 Angew. Chem., Int. Ed., 2015, 54, 2236.

528 (a) A. Chakraborty, J. Goura, P. Kalita, A. Swain, G. Rajaraman and V. Chandresekhar, Dalton Trans.,
529 2018, 47, 8841; (b) A. Upadhyay, C. Das, S. Vaidya, K. S. Sing, T. Gupta, R. Mondol, S. K.
530 Langley, K. S. Murray, G. Rajaraman and M. Shanmugam, Chem. – Eur. J., 2017, 23, 4903.

531 (a) A. Upadhyay, S. K. Singh, C. Das, R. Mondol, S. K. Langley, K. S. Murray, G. Rajaraman and M.
532 Shanmugam, Chem. Commun., 2014, 50, 8838; (b) N. F. Chilton, D. Collison, E. J. McInnes, R.
533 E. P. Winpenny and A. Soncini, Nat. Commun., 2013, 4, 2551; (c) J. D. Rinehart and J. R. Long,
534 Chem. Sci., 2011, 2, 2078; (d) C. Das, A. Upadhyay, S. Vaidya, S. K. Singh, G. Rajaraman and
535 M. Shanmugam, Chem. Commun., 2015, 51, 6137; (e) J.-L. Liu, Y.-C. Chen, Y.-Z. Zheng, W.-Q.
536 Lin, L. Ungur, W. Wernsdorfer, L. F. Chibotaru and M.-L. Tong, Chem. Sci., 2013, 4, 3310.

537 H.-R. Wen, S.-J. Liu, X.-R. Xie, J. Bao, C.-M. Liu and J.-L. Chen, Inorg. Chim. Acta, 2015, 435, 274.

(a) H. Zabrodsky, S. Peleg and D. Avnir, J. Am. Chem. Soc., 1992, 114, 7843; (b) J. Cirera, P. Alemany and S. Alvarez, Chem. – Eur. J., 2004, 10, 190; (c) M. Llunell, D. Casanova, J. Cirera, P. Alemany and S. Alvarez, SHAPE version 2.0, Barcelona, 2010. The program can be obtained by requesting with the authors.

G. Toth, S. G. Bowers, A. P. Truong and G. Probst, Curr. Pharm. Des., 2007, 13, 3476.

(a) H. Schmidt and D. Rehder, Inorg. Chim. Acta, 1998, 267, 229; (b) O. Margeat, P. G. Lacroix, J. P. Costes, B. Donnadieu, C. Lepetit and K. Nakatani, Inorg. Chem., 2004, 43, 4743; (c) W.-Y. Bi, X.-Q. Lu, W.-L. Chai, J.-R. Song, W.-Y. Wong, W.-K. Wong and R. A. Jones, J. Mol. Struct.,2008, 891, 450.

Y. Sui, D.-P. Li, C.-H. Li, X.-H. Zhou, T. Wu and X.-Z. You, Inorg. Chem., 2010, 49, 1286. 26 (a) N. C. Anastasiadis, C. M. Granadeiro, N. Klouras, L. Cunha-Silva, C. Raptopoulou, V. Psycharis, V. Bekiari, S. S. Balula, A. Escuer and S. P. Perlepes, Inorg. Chem., 2013, 52, 4145; (b) N. C. Anastasiadis, C. D. Polyzou, G. E. Kostakis, V. Bekiari, Y. Lan, S. P. Perlepes, K. K. Konidaris and A. K. Powell, Dalton Trans., 2015, 44, 19791; (c) X.-C. Huang, V. Vieru, L. F. Chibotaru, W. Wernsdorfer, S.-D. Jiang and X. Y. Wang, Chem. Commun., 2015, 51, 10373.

M. V. Marinho, D. O. Reis, W. X. C. Oliveira, L. F. Marques, H. O. Stumpf, M. Déniz, J. Pasán, C. Ruiz- Pérez, J. Cano, F. Lloret and M. Julve, Inorg. Chem., 2017, 56, 2108.

N. F. Chilton, R. P. Anderson, L. D. Turner, A. Soncini and K. S. Murray, J. Comput. Chem., 2013, 34, 1164.

(a) R. Sessoli, D. Gatteschi, A. Caneschi and M. A. Novak, Nature, 1993, 365, 141; (b) J. Villain, F. Hartman-Boutron, R. Sessoli and A. Rattori, Europhys. Lett., 1994, 27, 159.

J. M. Zadrozny, J. Liu, N. A. Piro, C. J. Chang, S. Hill and J. R. Long, Chem. Commun., 2012, 48, 3927.

R. Orbach, Proc. R. Soc. London, Ser. A, 1961, 264, 485.

J. Bartolomé, G. Filoti, V. Kuncser, G. Schienteie, V. Mereacre, C. E. Anson, A. K. Powell, D. Prodius and C. Turta, Phys. Rev. B: Condens. Matter, 2009, 80, 014430.

S. K. Singh, T. Gupta, L. Ungur and G. Rajaraman, Chem. – Eur. J., 2015, 21, 13812.

(a) J. D. Rinehart and J. R. Long, Dalton Trans., 2012, 41, 13572; (b) S. D. Gupta, T. Rajeshkumar, G. Rajaraman and R. Murugavel, Chem. Commun., 2016, 52, 7168.

(a) P.-H. Lin, W.-B. Sun, Y.-M. Tian, P.-F. Yan, L. Ungur, L. F. Chibotaru and M. Murugesu, Dalton Trans., 2012, 41, 12349; (b) M. A. Aldamen, S. Cardona-Serra, J. M. Clemente-Juan, E. Coronado, A. Gaita-Ariño, F. Martin-Gastaldo, F. Luis and O. Montero, Inorg. Chem., 2009, 48, 3467; (c) H. L. C. Feltham, F. Klower, S. A. Cameron, D. S. Larsen, Y. Lan, M. Tropiano, S. Faulkner, A. K. Powell and S. Brooker, Dalton Trans., 2011, 40, 11425; (d) M. Sugita, N. Ishikawa, T. Ishikawa, S. Koshinara and Y. Kaizu, Inorg. Chem., 2006, 45, 1299.

(a) K. S. Cole and R. H. Cole, J. Chem. Phys., 1941, 9, 341; (b) M. L. Kahn, J. P. Sutter, S. Golhen, P. Guionneau, L. Ouahab, O. Kahn and D. Chasseau, J. Am. Chem. Soc., 2000, 122, 3413.

G. Filoti, V. Kuncser, G. Schinteie, V. Mereacre, C. E. Anson, A. K. Powell, D. Prodius and C. Turta, Phys. Rev. B: Condens. Matter, 2009, 80, 014430–014431.

L. Escalera-Moreno, J. J. Baldovi, A. Gaita-Ariño and E. Coronado, Chem. Sci., 2018, 9, 3265.

A. Abragam and B. Bleaney, Electron paramagnetic resonance of transition ions, Dover Publications Inc., New York, 1970.

(a) P. E. Car, M. Perfetti, M. Mannini, A. Favre, A. Caneschi and R. Sessoli, Chem. Commun., 2011, 47, 3751; (b) M. Jeletic, P.-H. Lin, J. J. Le Roy, I. Korobkov, S. I. Gorelsky and M. Murugesu, J. Am. Chem. Soc., 2011, 133, 19286; (c) J. Ruiz, A. J. Mota, A. Rodriguez-Dieguez, S. Titos, J.-M. Herrera, E. Ruiz, E. Cremandes, J.-P. Costes and E. Colacio, Chem. Commun., 2012, 48, 7916.

M. M. Hanninen, A. J. Mota, D. Aravena, E. Ruiz, R. Sillanpaa, A. Camon, M. Evangelisti and E. Colacio, Chem. – Eur. J., 2014, 20, 8410.

N. F. Chilton, D. Collison, E. J. L. McInnes, R. E. P. Winpenny and A. Soncini, Nat. Commun., 2013, 4, 2551.

Legends to figures

Scheme 1 Structural formula of the H2L ligand. Asterisks denote the chiral centres.

Figure. 1 Powder X-ray spectra of the [NiIILnIII] series of complexes 3–7. (*) indicates the spectrum calculated from the single crystal data of the [NiIIEuIII] complexes 1.

Figure. **2** Powder X-ray spectra of the [ZnIILnIII] series of complexes 8–12. The spectra plotted in black, bold (*) was calculated from the single crystal data of the [ZnIIEuIII] structure 2SSc. Simulated spectra from single crystal structures 2SS and 2SSb are shown below those from 2SSc.

Figure. **3** Top, spacefill mirror image of the enantiomeric 1RR and 1SS complexes. Down, ideal coordination polyhedron vs. real O-donor sites for the EuIII cation and partially labelled plot of complex 1RR. Colour key for all figures: ZnII firebrick, NiII green, EuIII orange, O red, N navy, C grey.

Figure. **4** CH–π(ring) interactions between the dinuclear [NiIIEuIII] complexes 1 that determine its 1-D arrangement in the network.

Figure. **5** Top, partially labelled plot of the molecular structure of complex 2SS. Bottom, 1D arrangement of dinuclear units linked by H-bonds mediated by the crystallization methanol molecules. Phenyl rings and methoxy groups have been suppressed for clarity.

Figure. **6** 1D arrangement of dinuclear units linked by H-bonds mediated by the crystallization methanol molecules alternated with direct H-bonds for 2SSb. Phenyl rings and methoxy groups have been suppressed for clarity.

Figure. **7** Top, partially labelled plot of the molecular structure of complex 2SSc. Down, ideal coordination polyhedron vs. real O-donor sites for the EuIII cation and regular 1D arrangement of dinuclear units linked by direct H-bonds. Phenyl rings and methoxy groups have been suppressed for clarity.

Figure. **8** Conformations of the phenyl rings for the L2− ligand: in plane for the coordinated ZnII (left) and perpendicular for the NiII (right).

Figure. **9** Solution ECD spectra for the NiIIEuIII pair of complexes 1RR and 1SS (top) and the ZnIIEuIII pair 2RR, 2SS (bottom). (R,R) enantiomers, red lines; (S,S) enantiomers, blue lines.

626 **Figure**. **10** Dependence of out-of-phase susceptibility for complexes 3–7 and 8–11 measured under a dc
627 field of 500 Oe for 3 and 8 and 1000 Oe for the remaining complexes. Temperature range 2–10 K.
628
629 **Figure**. **11** A view of the charged O-donors "belt" around the LnIII ions and the axial neutral O-donors
630 (left). Plot of the anisotropy axis cations (green lines, Magellan program)42 calculated for the
631 [NiIIDyIII] (center) and [ZnIIDyIII] (right) showing that the distribution of the charge around the
632 lanthanide is more adequate for the prolate-like lanthanides.
633
634
635

636 **SCHEME** 1

637

638

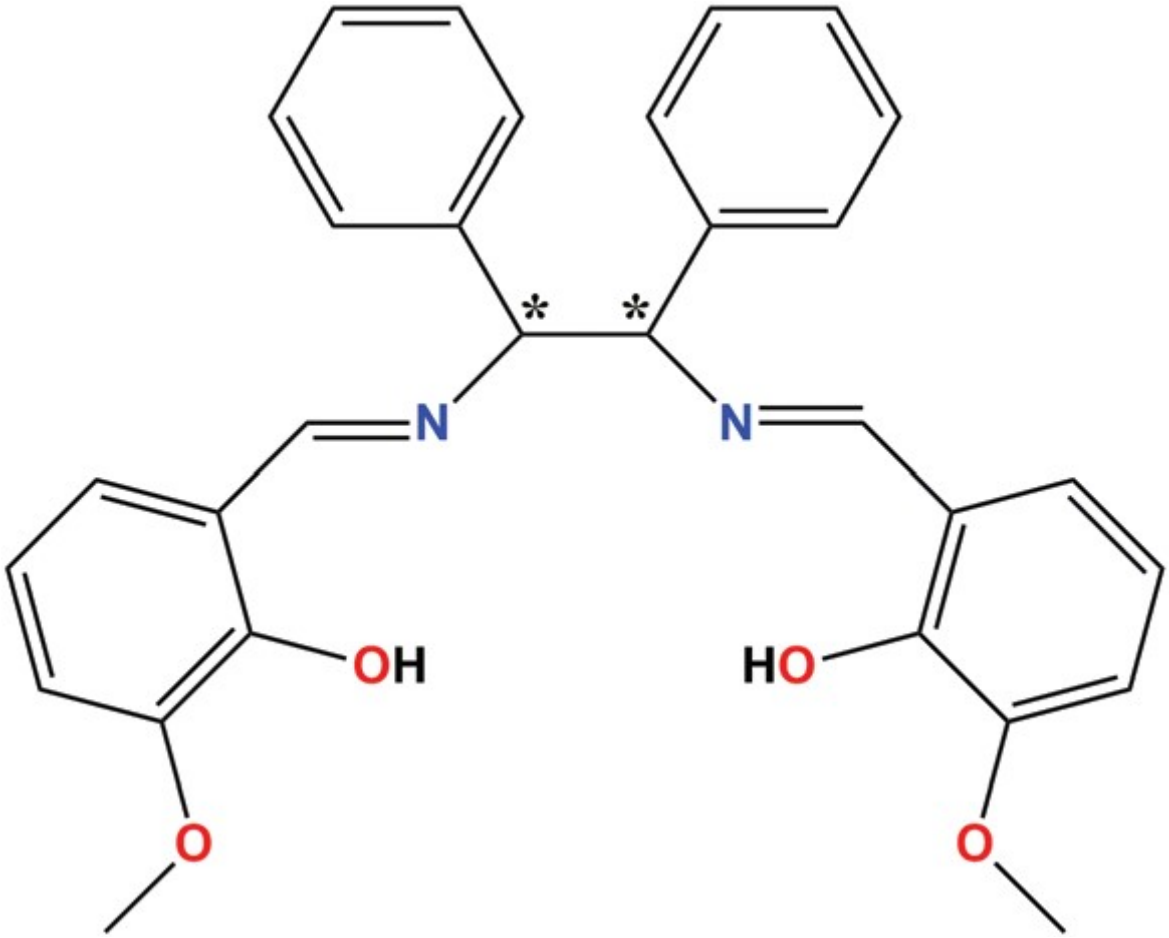

639

640

641 **FIGURE 1**

642

643

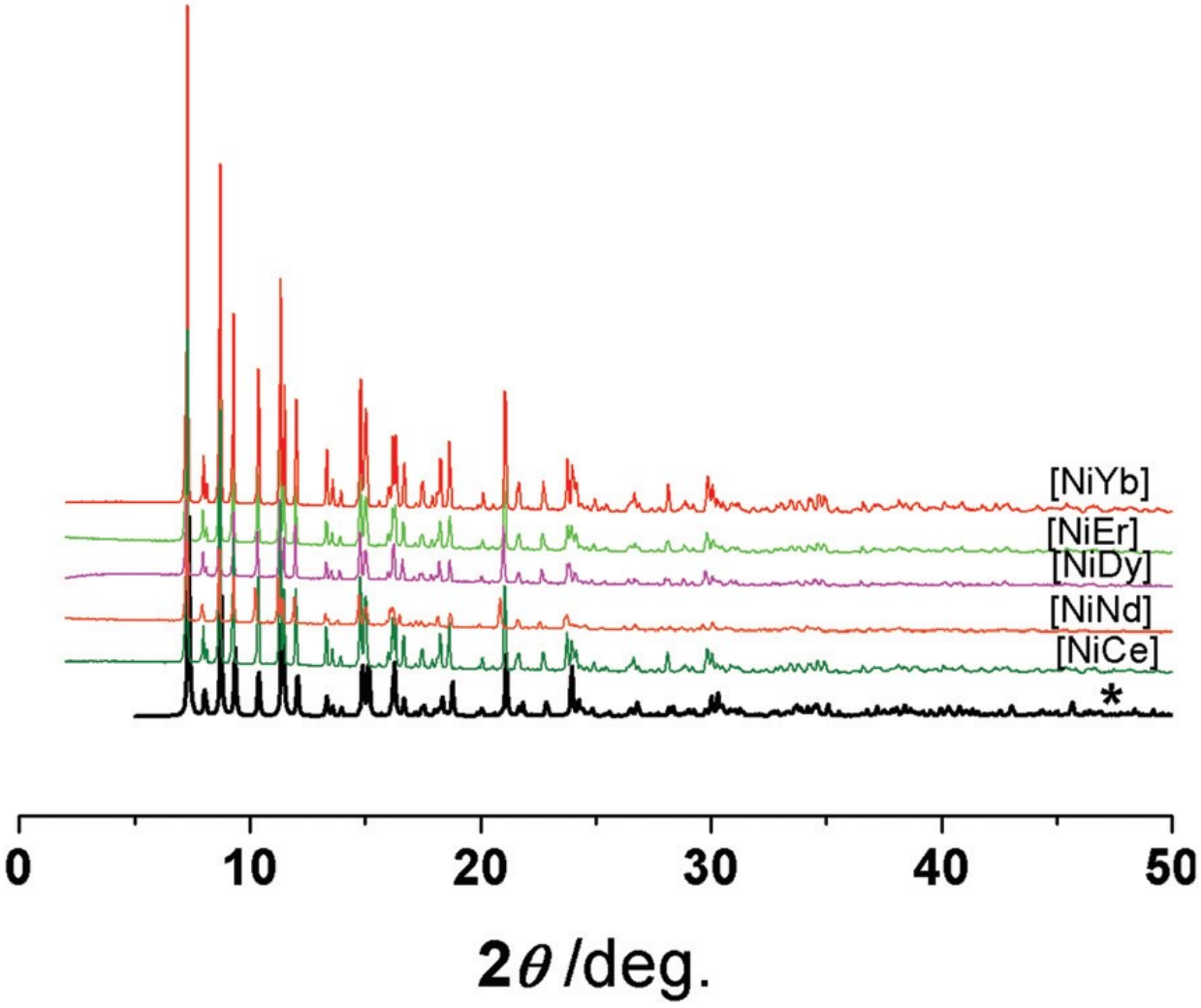

644

645

646 **FIGURE 2**

647

648

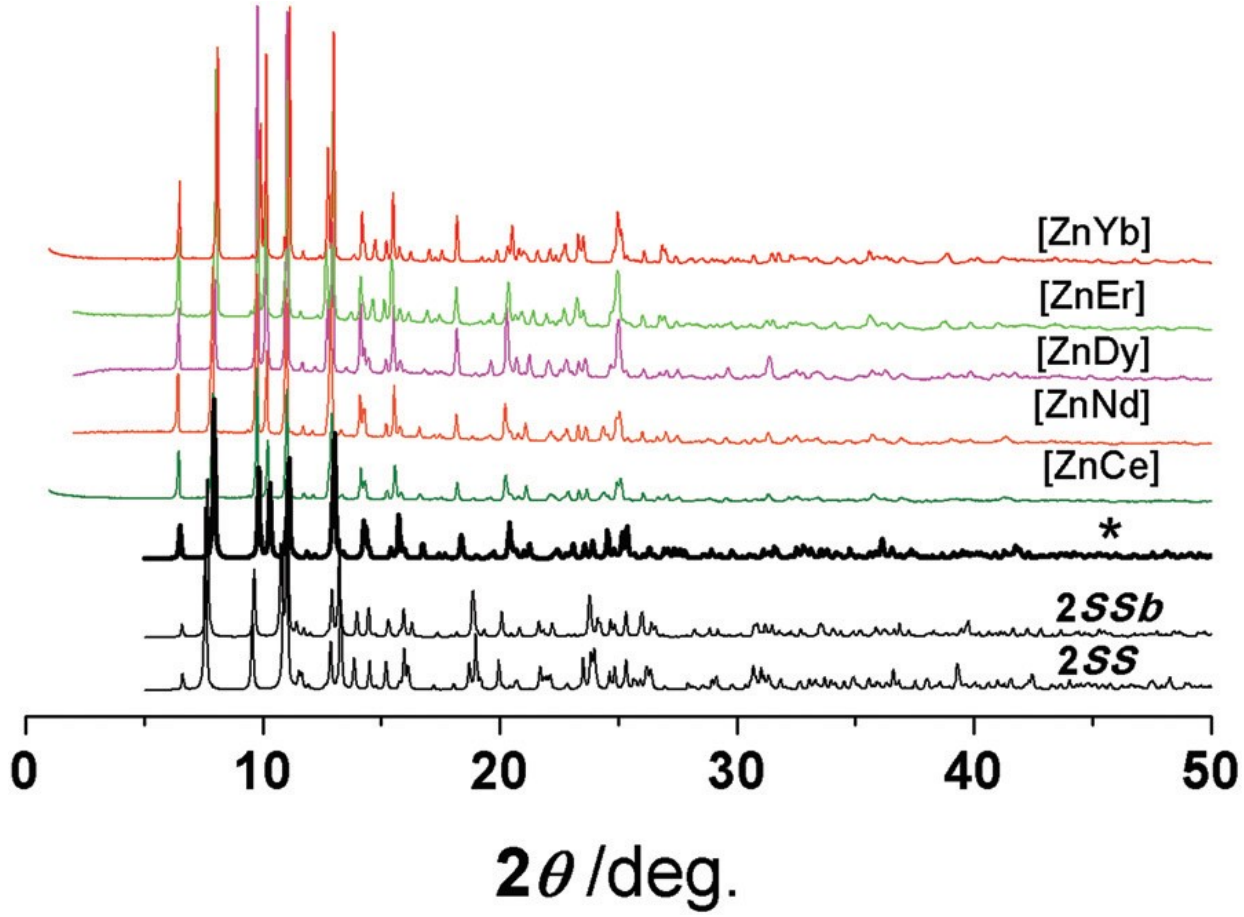

649

650

651 **FIGURE** 3

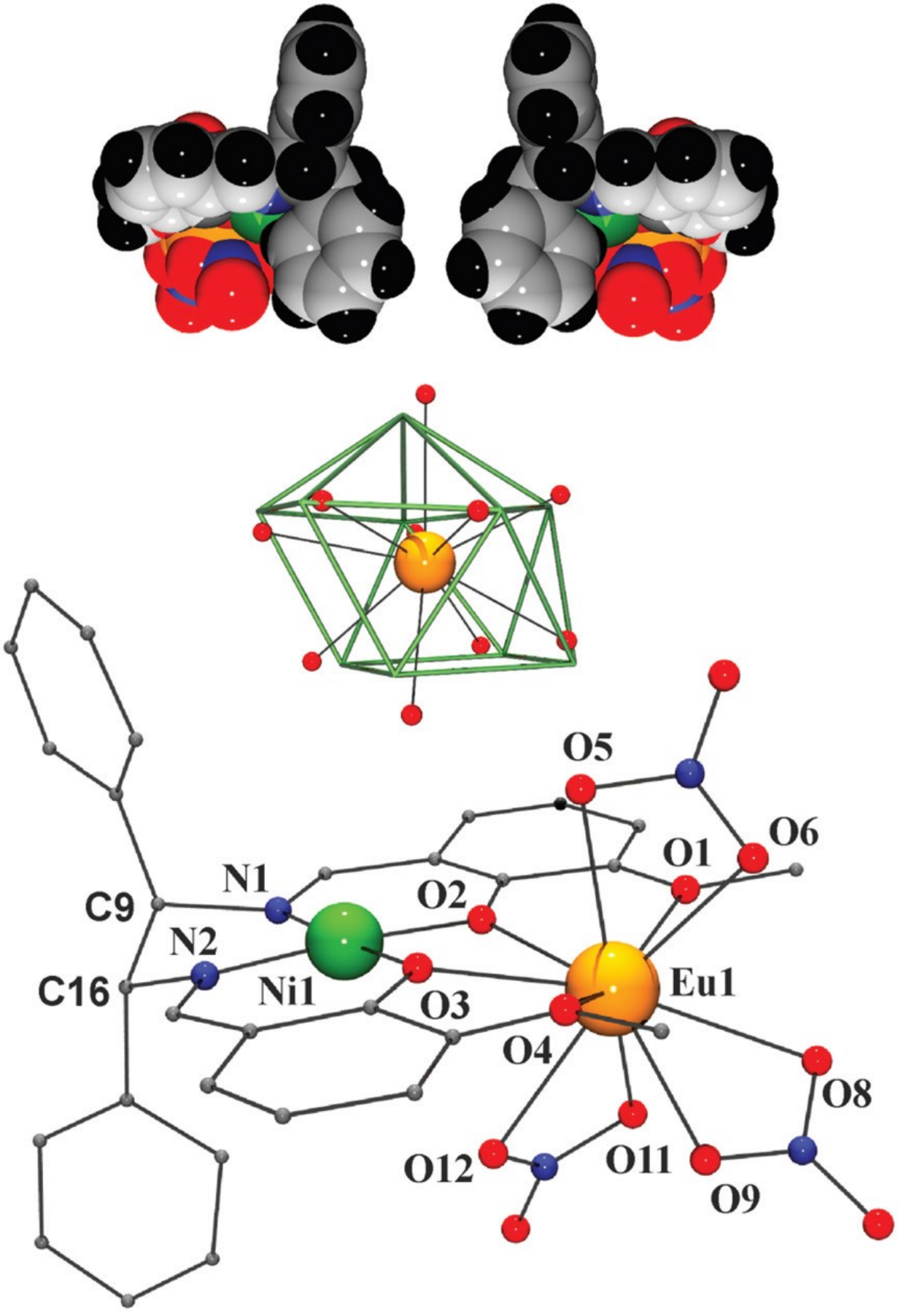

652
653

654 **FIGURE 4**

655

656

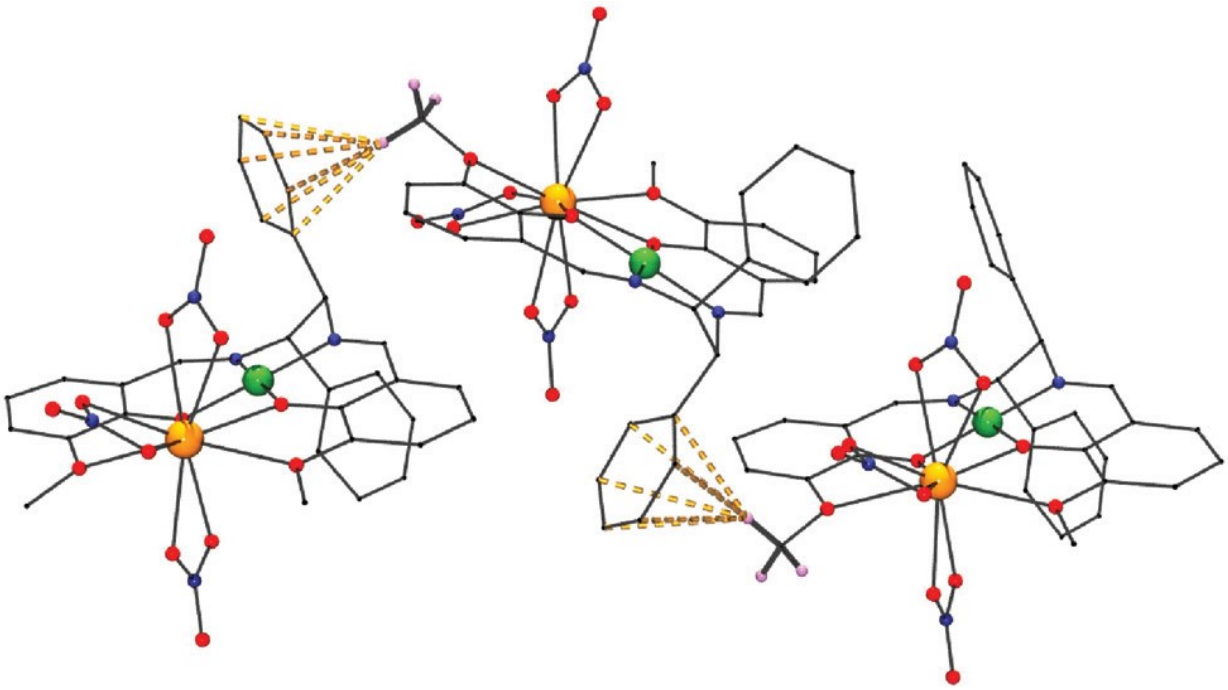

657

658

FIGURE 5

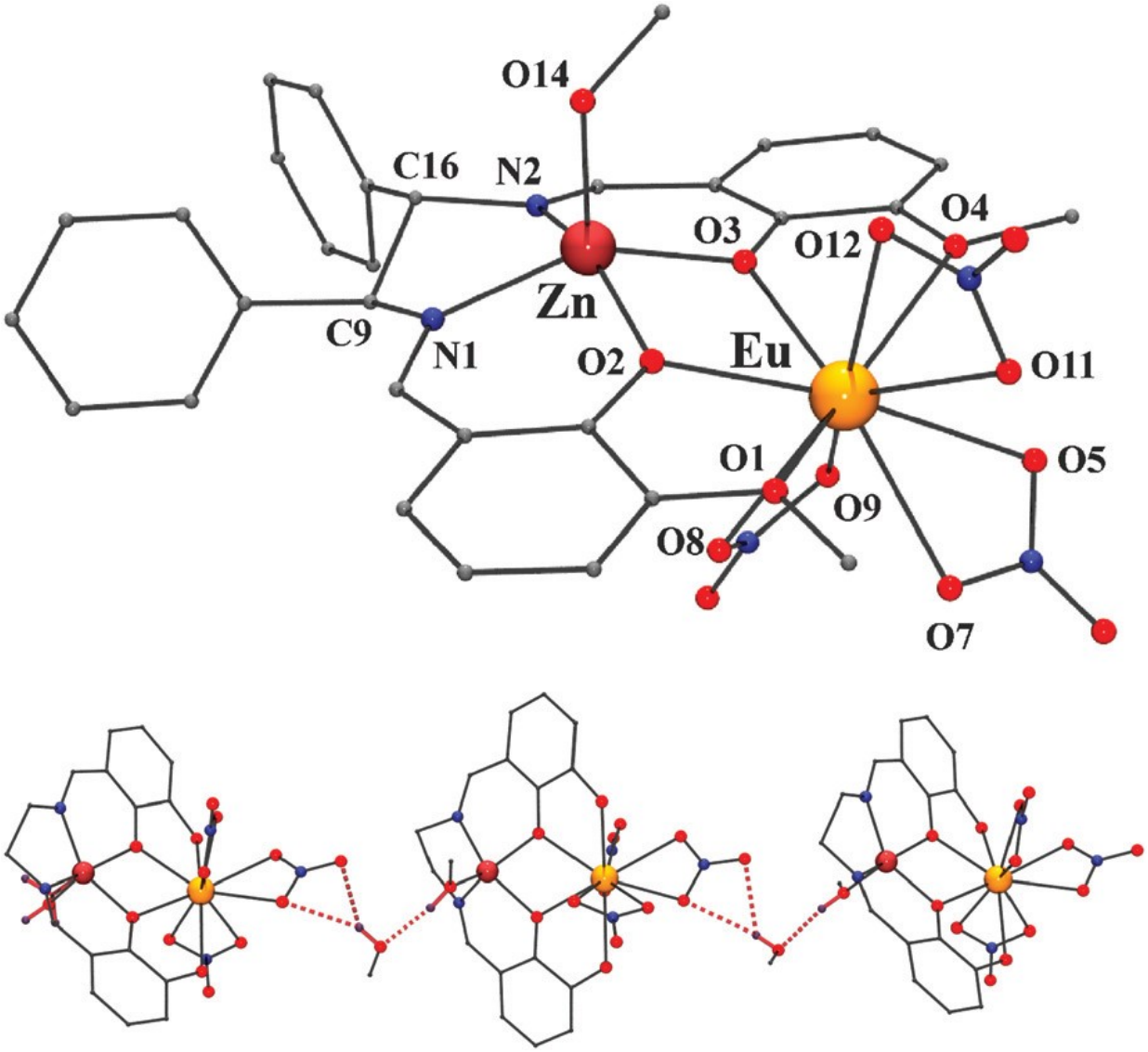

FIGURE 6

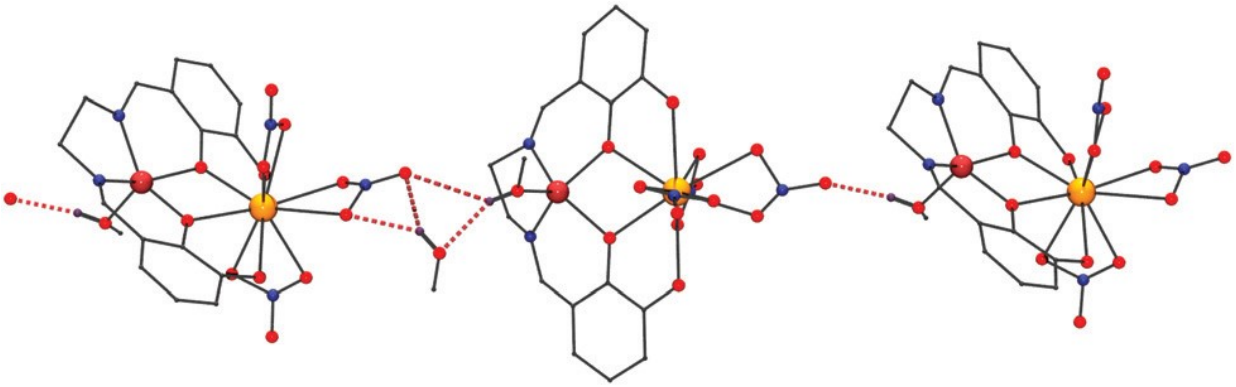

672 **FIGURE 7**

673

674

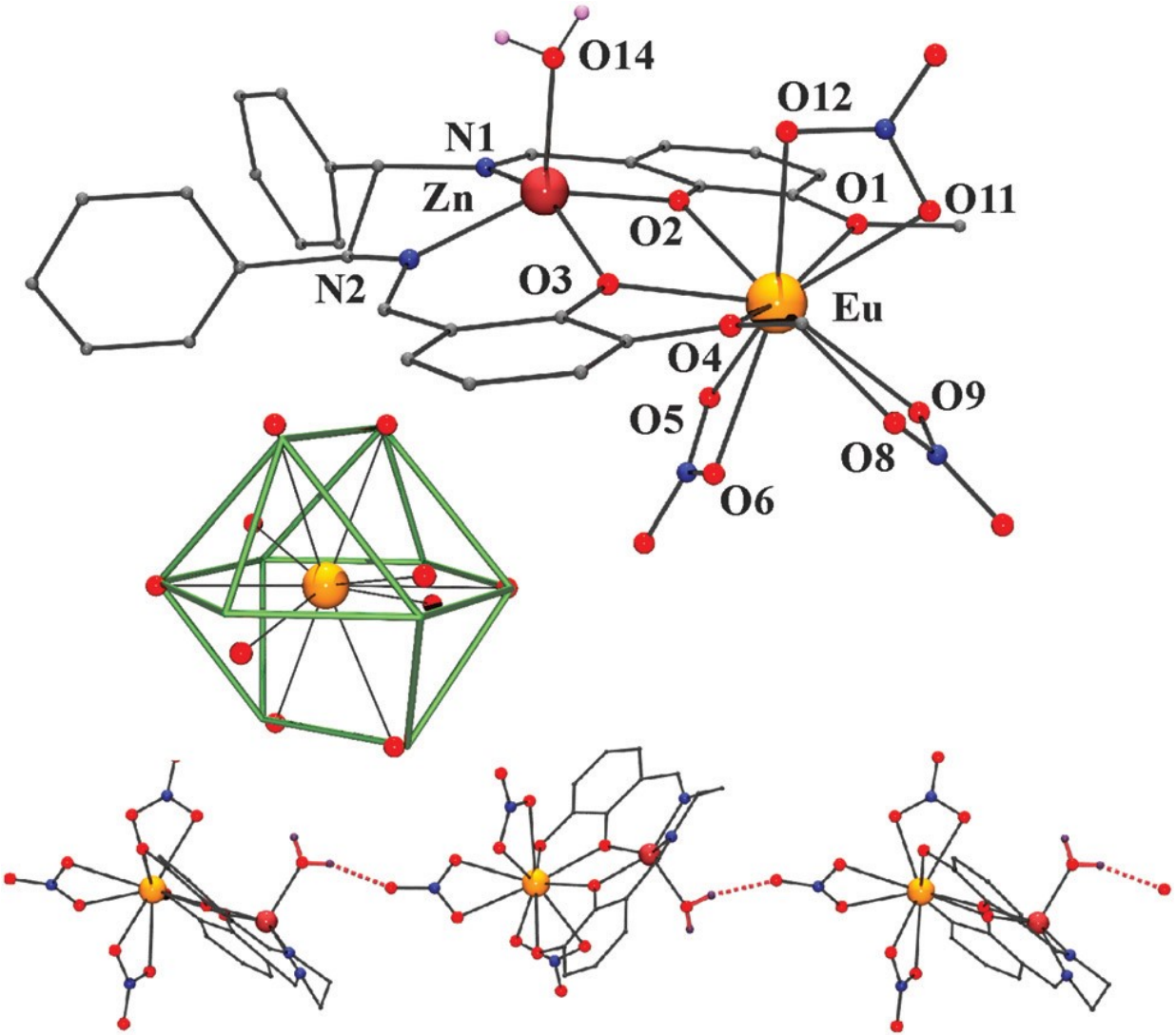

675

676

677 **FIGURE 8**

678

679

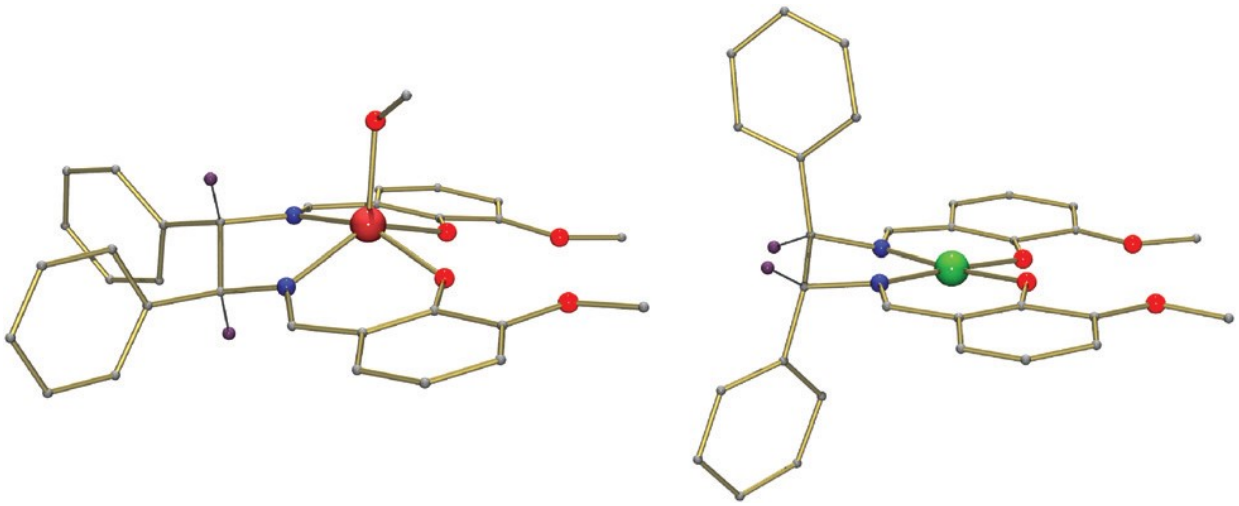

680

681

682

683 **FIGURE 9**

684

685

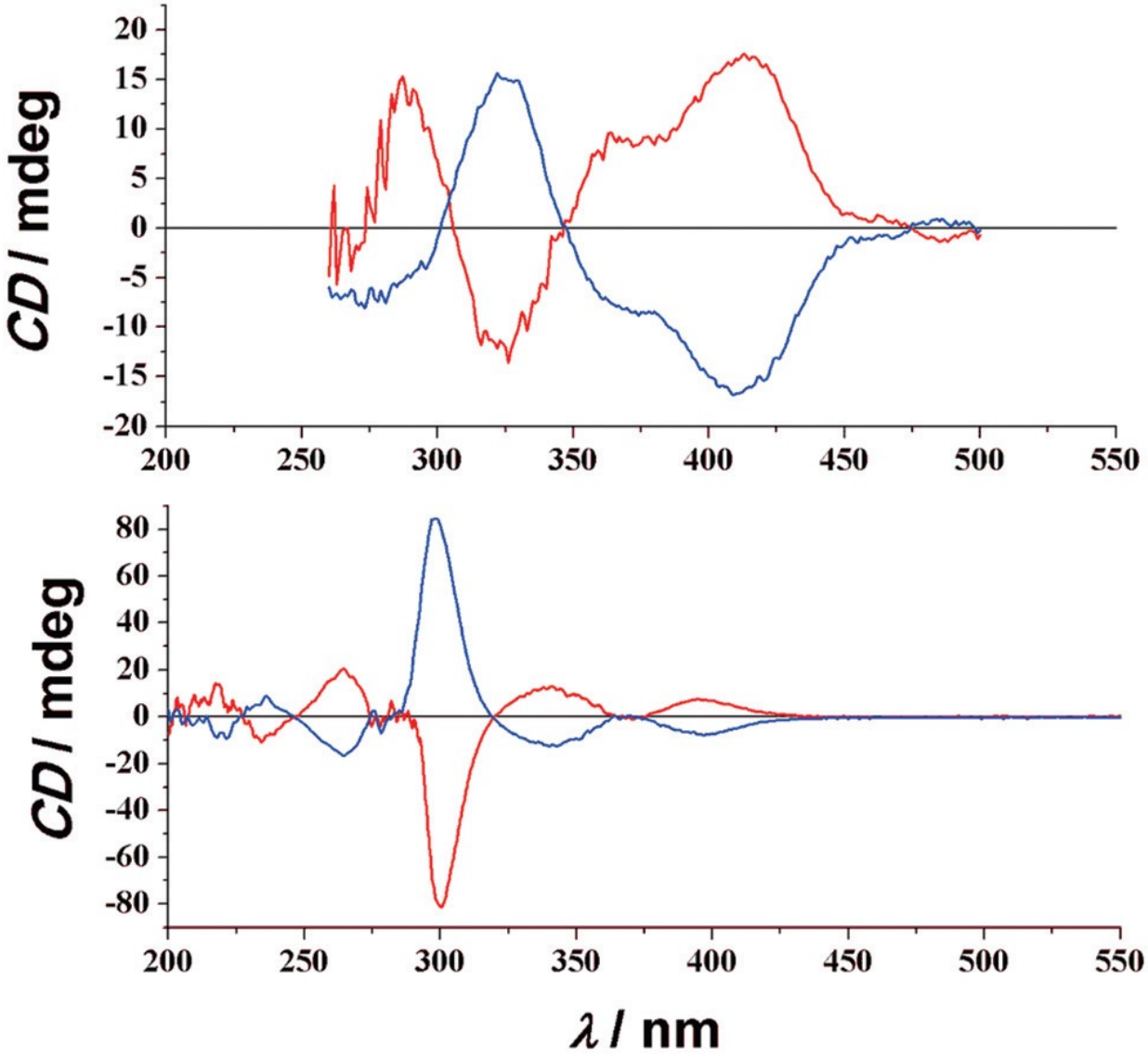

686

687

688 **FIGURE 10**

689

690

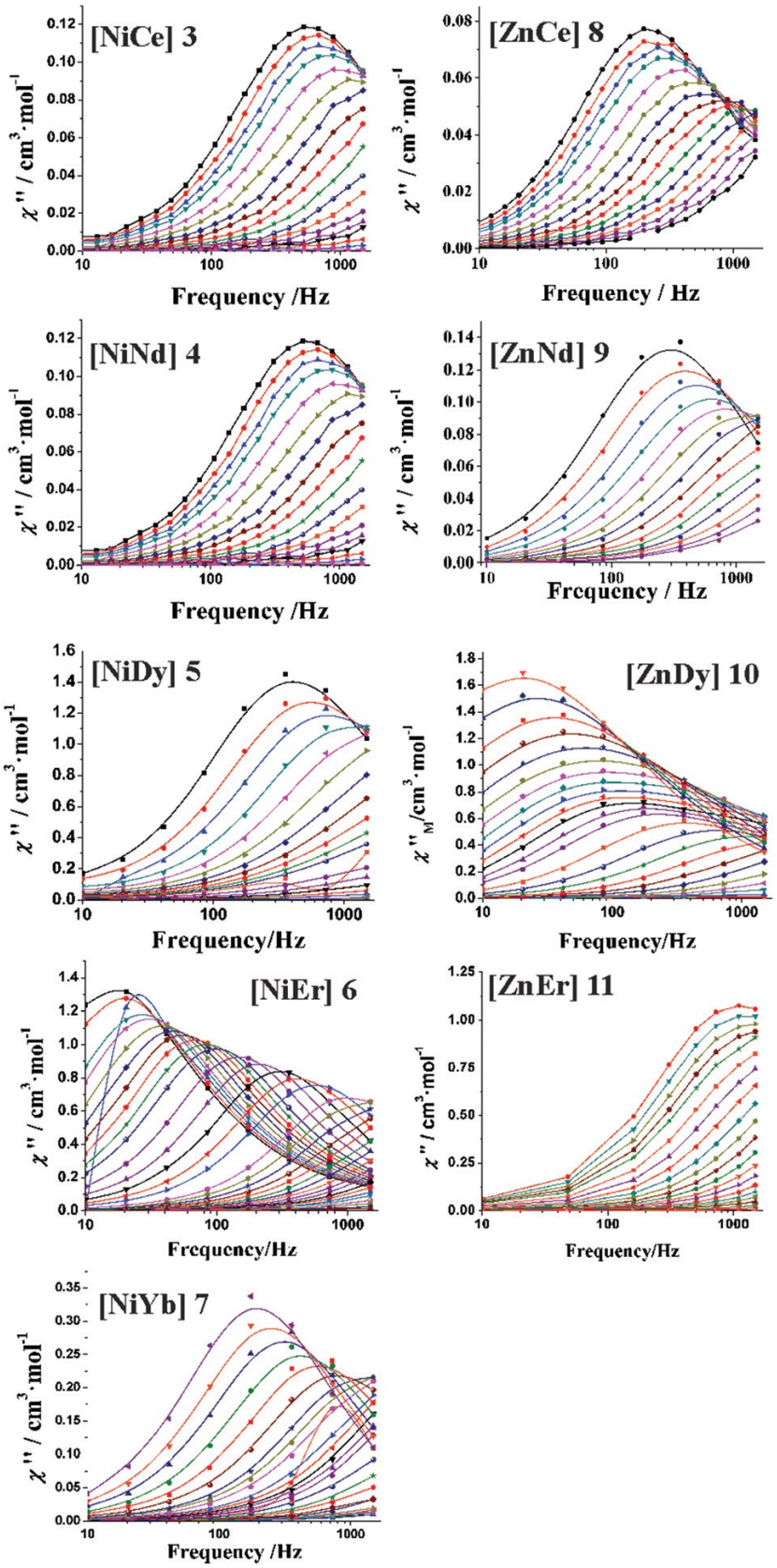

691

692

693 **FIGURE 11**

694

695

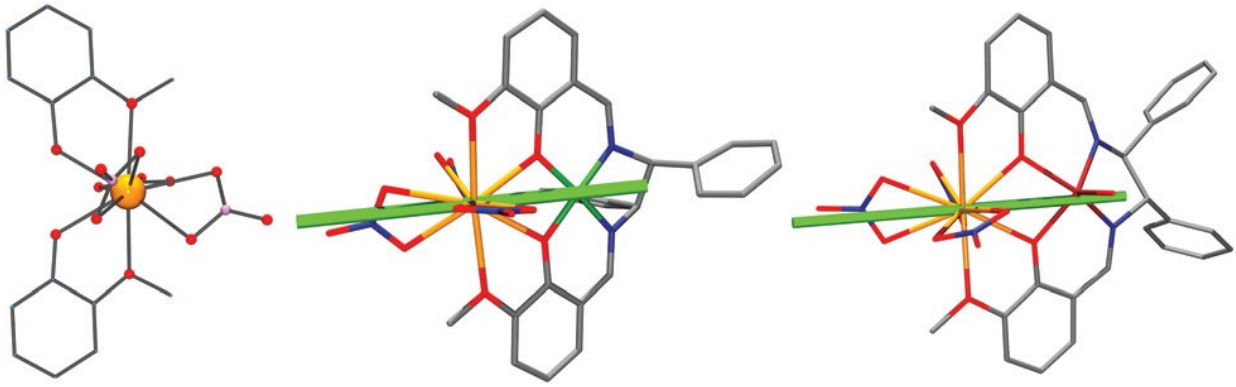

696

697

698 **Table 1** Selected bond distances (Å) and angles (°) for the A-molecule of 1RR

699

Eu(1)–O(1)	2.552(7)	Ni(1)–N(1)	1.806(7)
Eu(1)–O(2)	2.389(6)	Ni(1)–N(2)	1.840(6)
Eu(1)–O(3)	2.417(4)	Ni(1)–O(2)	1.838(6)
Eu(1)–O(4)	2.550(6)	Ni(1)–O(3)	1.843(6)
Eu(1)–O(5)	2.504(6)	Ni(1)–O(2)–Eu(1)	106.7(3)
Eu(1)–O(6)	2.421(5)	Ni(1)–O(3)–Eu(1)	105.4(2)
Eu(1)–O(8)	2.593(6)	Ni(1)···Eu(1)	3.406(1)
Eu(1)–O(9)	2.480(6)		
Eu(1)–O(11)	2.472(6)		
Eu(1)–O(12)	2.538(5)		

700

701

Table 2 Selected bond distances (Å) and angles (°) for the A-molecule of 2SS

Eu(1)–O(1)	2.703(4)	Zn(1)–N(1)	2.045(4)
Eu(1)–O(2)	2.337(3)	Zn(1)–N(2)	2.020(4)
Eu(1)–O(3)	2.368(3)	Zn(1)–O(2)	1.981(3)
Eu(1)–O(4)	2.608(3)	Zn(1)–O(3)	1.991(4)
Eu(1)–O(5)	2.543(4)	Zn(1)–O(14)	2.006(4)
Eu(1)–O(7)	2.568(4)	Zn(1)–O(2)–Eu(1)	108.2(1)
Eu(1)–O(8)	2.487(6)	Zn(1)–O(3)–Eu(1)	106.6(1)
Eu(1)–O(9)	2.469(5)	Zn(1)···Eu(1)	3.503(1)
Eu(1)–O(11)	2.446(4)		
Eu(1)–O(12)	2.505(4)		

706 **Table 3** Selected bond distances (Å) and angles (°) for the A-molecule of 2SSc

707

Eu(1)–O(1)	2.606(7)	Zn(1)–N(1)	1.98(1)
Eu(1)–O(2)	2.380(7)	Zn(1)–N(2)	2.067(7)
Eu(1)–O(3)	2.348(6)	Zn(1)–O(2)	1.988(7)
Eu(1)–O(4)	2.693(8)	Zn(1)–O(3)	1.995(8)
Eu(1)–O(5)	2.454(9)	Zn(1)–O(14)	1.990(9)
Eu(1)–O(6)	2.444(9)	Zn(1)–O(2)–Eu(1)	106.8(3)
Eu(1)–O(8)	2.537(9)	Zn(1)–O(3)–Eu(1)	107.8(3)
Eu(1)–O(9)	2.554(8)	Zn(1)···Eu(1)	3.515(1)
Eu(1)–O(11)	2.47(1)		
Eu(1)–O(12)	2.52(1)		

708

709

710 **Table 4** Slow relaxation of the magnetization parameters for complexes 3–7 and 8–12

711

Complex	U_{eff} (K)	τ_0 (s)	Complex	U_{eff} (K)	τ_0 (s)
[NiCe] **3**	8.5[a]	7.7×10^{-5}	[ZnCe] **8**	4.7[b]	2.5×10^{-5}
[NiNd] **4**	9.2[a]	1.9×10^{-5}	[ZnNd] **9**	15.9[a]	3.7×10^{-6}
[NiDy] **5**	9.3[a]	2.1×10^{-5}	[ZnDy] **10**	17.7[b]	8.3×10^{-7}
[NiEr] **6**	18.4[b]	1.7×10^{-6}	[ZnEr] **11**	—	—
[NiYb] **7**	18.1[a]	2.1×10^{-6}	[ZnYb] **12**	—	—

[a] Generalized Debye model fit. [b] Arrhenius fit.

712